We have studied these three polyribonucleotide complexes[19] in aqueous solution by ^{31}P NMR spectroscopy (80.6 MHz) above (spectra not shown) and below the thermal denaturation temperature (T_m) (Figure 1) of the helical complex. Above the T_m, the spectral lines are generally sharp ($\Delta\nu_{1/2} < 2$ Hz) and consist of one or two resonances of expected intensity,[22] reflecting the homopolymer stoichiometry of the respective complexes. Below the T_m (Figure 1), the resonances are somewhat broader ($\Delta\nu_{1/2} \sim 20$–50 Hz), presumably reflecting effects due to reduced correlation times of the phosphates of the base-paired complexes. Additional features of the spectra of these complexes are as follows: (a) poly(A^+)·poly(A^+) has *one* phosphorus resonance;[23] (b) poly(A)·poly(U) has *two* resonances of approximately equal intensity; (c) poly(A)·2poly(U) has *three* resonances, each of approximately equal intensity. The chemical shift positions of the resonances of these and additional polynucleotide complexes are listed in Table I. An unanticipated feature of these spectra is the observation of multiple resonances in three of the double-stranded helical complexes [poly(A)·poly(U), poly(I)·poly(C), and poly(I)·poly(C_{12}U)].[25] Plausible explanations for the observation of more than one resonance are (1) two equal populations of helical complexes having different phosphate-backbone conformations, each having C_2 symmetry with an exchange rate slow on the NMR time scale, (2) a single helical complex having C_2 symmetry but containing local phosphate magnetic anisotropy[27] (e.g., due to solution environment[30]), and (3) a single helical complex where the two strands have different phosphate-backbone conformations. Various studies of these complexes (effects of temperature, ionic strength, RNA–DNA hybrid complexes) do not support the first explanation[32] and provide tentative assignments[33] of some of the base-paired resonances in Table I. The second and third explanations are both considered possible contributors to the multiple resonances observed. Our collective results from these complexes in various salts[35] of poly(A)·2poly(U) at conditions where the triple-to-double-stranded conversion occurs, and the observed three resonance pattern of poly(A)·2poly(U) anticipated from the unique strand conformations of the fiber,[18a] strongly suggest that the third explanation (strands with different phosphate-backbone conformations) is a reasonable contributor to the multiple resonances observed in these complexes. Additional experiments are necessary to unequivocally assign the resonances to specific strands and to determine the relative contributions of mechanisms 2 and 3 to the observed chemical shifts. However, irrespective of the explanation of the resonance multiplicity, these results illustrate the utility of the ^{31}P NMR technique for probing the phosphate backbone of individual strands in helical complexes.

Acknowledgment. We acknowledge the National Science Foundation and National Institutes of Health (CA-25438) for support in purchasing the NMR spectrometer and Franklyn Wissler for performing the ring-current calculations.

(19) Polynucleotide complexes were prepared as previously described.[20] These complexes were sonicated by using a Branson Sonifier (Model W185; equipped with a tapered micro tip) at 0 °C under nitrogen atmosphere. Integrity of the complex was determined by using thermal denaturation profile (UV spectroscopy) before and after sonication, and after sonication the complex had a broad molecular weight distribution as determined from polyacrylamide gel electrophoresis (7.5%) in 40 mM Tris acetate (pH 8.0). The size was generally greater than 150 base pairs, using the Hae III restriction fragments of PM2 DNA as comparative size markers.[21]

(20) Carter, W. A.; Pitha, P. M.; Marshall, L. W.; Tazawa, I.; Tazawa, S.; Ts'o, P. O. P. *J. Mol. Biol.* **1972**, *70*, 567–587.

(21) Kovacie, R. T.; van Holde, K. E. *Biochemistry* **1977**, *16*, 1490–1498.

(22) Spectra are acquired by using conditions where accurate resonance intensities can be obtained. An inverted-gated decoupling (proton decoupling without NOE enhancement) acquisition scheme is used on a WP-200 NMR spectrometer. Pulse repetition rates of ≥10 s and flip angles of ≤36° are utilized.

(23) A similar observation has recently been reported.[24]

(24) Lerner, D. B.; Kearns, D. R. *Biopolymers* **1981**, *20*, 803–806.

(25) In the alternating copolymer poly(I-C), two phosphorus resonances have been observed[26] (−4.48 and −4.25 ppm, 35.5 °C). The difference in these resonances ($\Delta\delta$ 0.23) is about one-half that observed (Table I) for poly(I)·poly(C) ($\Delta\delta = 0.51$). The smaller $\Delta\delta$ for poly(I-C) does not appear due to line-width differences since they are not symmetrically positioned between the resonances of poly(I)·poly(C). The two resonances in poly(I-C) may reflect sequence variations in the sugar-phosphate-backbone conformation.

(26) Patel, D. J. In "Nucleic Acid Geometry and Dynamics"; Sarma, R. H., Ed.; Pergamon Press: New York, 1980; pp 185–231.

(27) A reasonable contributor here might be ring-current anisotropy from different base moieties on the phosphates of the individual strands. Ring-current calculations have been made for homopolymers in the A-RNA conformation[28] by using the equivalent dipole model.[29] The chemical shift difference ($\Delta\delta$) of the phosphates of different strands is 0.09 ppm for poly(A)·poly(U) and 0.05 ppm for poly(I)·poly(C). While it is apparent ring-current anisotropy may contribute to chemical shift differences, this calculated effect is not sufficient to account for the observed results.

(28) Arnott, S.; Hukins, D. W. L. *Biochem. Biophys. Res. Commun.* **1972**, *48*, 1392–1399.

(29) Abraham, R. J. in "Nuclear Magnetic Resonance Spectroscopy in Molecular Biology"; Pullman, B., Ed.; D. Reidel: Dordrecht, Holland, 1978; pp 461–479.

(30) Solute–solvent interactions[31] or specific interactions mediated by the base moiety (e.g., guanine·Mg^{2+}·H_2O·phosphate[10c]) could generate anisotropy.

(31) Lerner, D. B.; Kearns, D. R. *J. Am. Chem. Soc.* **1980**, *102*, 7611–7612.

(32) In all cases (Table I) where multiple resonances are observed, their intensities disappear at essentially the same rate on going through the thermal denaturation temperature and reappear at the same rate on renaturation; this is also observed for poly(I)·poly(C) and poly(I)·poly(C_{12}U) at NaCl concentrations between 0–0.6 M and for poly(A)·poly(U) at low salt concentrations.

(33) (a) The poly(I)·poly(C) helical resonances are assigned by comparison to poly(dI)·poly(C) (−4.27 and −4.66 ppm) by assuming the two resonances most similar in chemical shift are those from the RNA strand. (b) In poly(A)·2poly(U), the Hoogstein base-paired poly(U) strand (lowest field resonance) was assigned by comparison of the poly(A)·poly(U) and poly(A)·2poly(U) spectra and by a temperature study of poly(A)·2poly(U) at low salt where the 3 → 2 + 1 stranded conversion[34] occurs. At this condition the lowest field resonance disappeared and reappeared as a sharp line with a chemical shift expected for free poly(U), while the intensity of the other two higher-field resonances remained constant.

(34) Stevens, C. L.; Felsenfeld, G. *Biopolymers* **1964**, *2*, 293–314.

(35) In the case of poly(I)·poly(C), similar results are obtained in the presence or absence of added NaCl or in the presence of added $MgCl_2$.

Reaction between HO_2· and Chlorine in Aqueous Solution

E. Bjergbakke

Risø National Laboratory
DK-4000, Roskilde, Denmark

S. Navaratnam and B. J. Parsons

School of Natural Sciences, Kelsterton College
North E. Wales Institute, Connah's Quay
Clwyd, CH5 4BR, United Kingdom

A. J. Swallow*

Paterson Laboratories,
Christie Hospital and Holt Radium Institute
Manchester M20 9BX, United Kingdom

Received May 1, 1981

Reactions in aqueous solution containing ferrous sulfate are among the best understood of radiolytic reaction mechanisms, but hitherto unsuspected reactions must be taking place when large radiation doses are applied instantaneously in the presence of added chloride.[1] We have recently found indications that yields under these conditions might be explicable if HO_2· radicals reduce Cl_2.[2] This communication reports independent confirmation of this reaction, obtained in a system designed to demonstrate it.

(1) Navaratnam, S.; Parsons, B. J.; Swallow, A. J. *Radiat. Phys. Chem.* **1980**, *15*, 159.

(2) Bjergbakke, E.; Navaratnam, S.; Parsons, B. J.; Swallow, A. J., manuscript in preparation.

(3) Gilbert, C. W.; Ingalls, R. B.; Swallow, A. J. *Radiat. Phys. Chem.* **1977**, *10*, 221.

(4) Jayson, G. G.; Parsons, B. J.; Swallow, A. J. *J. Chem. Soc., Faraday Trans. 1* **1973**, *69*, 1597.

(5) Swallow, A. J. "Radiation Chemistry"; Longman: London, 1973.

(6) Hasegawa, K.; Neta, P. *J. Phys. Chem.* **1978**, *82*, 854.

(7) Scott, R. L. *J. Am. Chem. Soc.* **1953**, *75*, 1550.

0002-7863/81/1503-5926$01.25/0

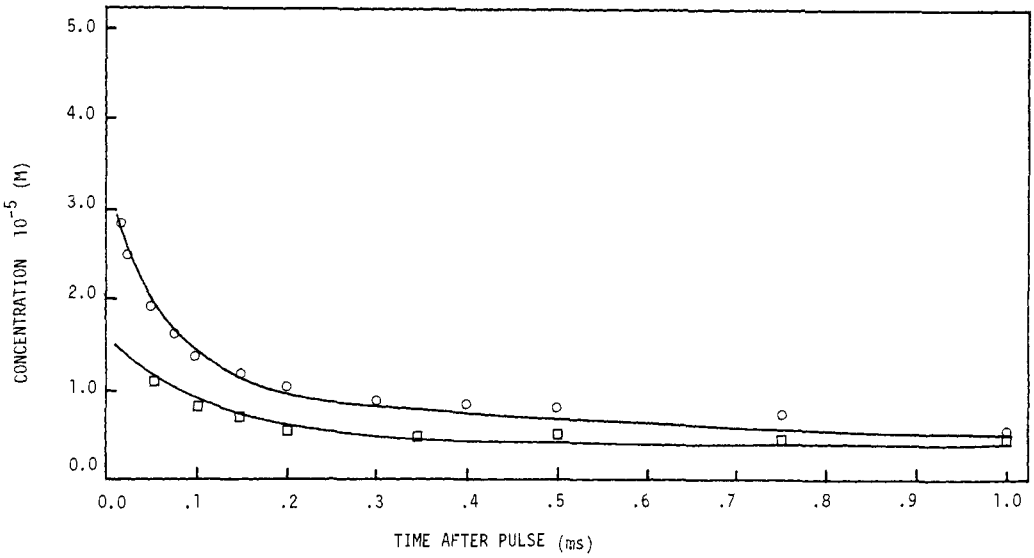

Figure 1. Decay of $HO_2\cdot$ in a pulse-irradiated (1 μs), oxygenated aqueous solution containing 0.19 M NaCl and 0.01 M $HClO_4$. (○) 93 Gy; (□) 40.1 Gy. The full lines show the calculated curves based on Table I and $k(HO_2\cdot + Cl_2) = 1.0 \times 10^9$ M^{-1} s^{-1}.

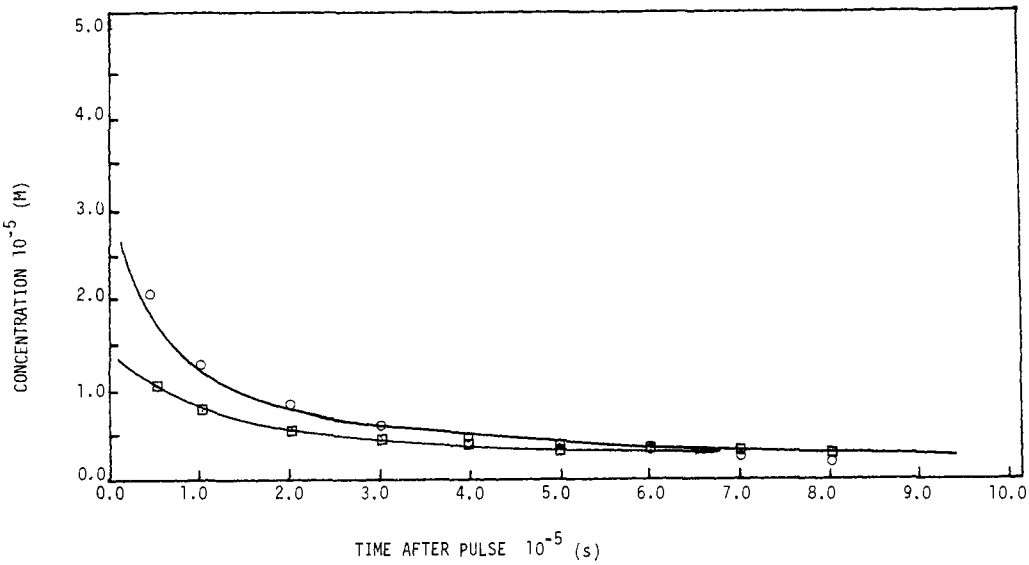

Figure 2. Decay of $Cl_2^-\cdot$ in a pulse-irradiated (1 μs), oxygenated aqueous solution containing 0.19 M NaCl and 0.01 M $HClO_4$. (○) 93 Gy; (□) 40.1 Gy. The full lines show the calculated curves based on Table I and $k(HO_2\cdot + Cl_2) = 1.0 \times 10^9$ M^{-1} s^{-1}.

Microsecond pulses (40.1 and 93.0 Gy) of fast electrons have been delivered to oxygen-saturated solutions containing NaCl (0.19 M) and $HClO_4$ (1.0×10^{-2} M). Known reactions of the primary species ·OH, H·, H_2, and H_2O_2, taken to be produced under our conditions with $G = 3.1$, 3.75, 0.4, and 0.7, respectively, are given in Table I (1–17). Of these reactions, 7, 12, and 13 are the most significant after the pulse. It may be noted that the hydrolysis of chlorine to HOCl[8] need not be considered as it is too slow. The concentration of $HO_2\cdot$ was calculated from optical absorption measurements made at 260 nm taking[9] ϵ 540 M^{-1} cm^{-1} and allowing for a contribution at that wavelength from $Cl_2^-\cdot$. The concentration of $Cl_2^-\cdot$ was calculated from measurements at 340 nm assuming[4] ϵ 8.8×10^3 M^{-1} cm^{-1}.

Measured variations in the concentrations of $HO_2\cdot$ and $Cl_2^-\cdot$ with time after the pulse are given in Figures 1 and 2. In order to fit the mechanism to the experimental data of Figure 1, sets of differential equations were integrated numerically on the Burroughs B6700 computer at Risø by using an algorithm originally developed by Gear for "stiff" systems[10] and subsequently applied to systems like the present one.[11] It became immediately clear that if reactions of Cl_2 (and Cl_3^-) were not included, approximately two-thirds of the initial $HO_2\cdot$ would remain after about 100 μs, disappearing only over a much longer time scale by mutual reaction. Since this does not fit the experimental data, reactions 18 and 19 may be considered. Variation in the rate constant for reaction 18 outside the limits 9×10^8 and 1.5×10^9 M^{-1} s^{-1} could not give good fits, but a good fit was obtained with 1.0×10^9 M^{-1} s^{-1}. The rate constant for reaction 19 was taken to be identical with that for reaction 18, but even with this high value the reaction had little effect on the decay of $HO_2\cdot$.

An additional possibility considered was that $HO_2\cdot$ might react with $Cl_2^-\cdot$ to produce Cl_2 and H_2O_2. This reaction was therefore included in the mechanism in addition to reaction 13. From the computations it was seen that if the reaction had a high rate constant it would provide an efficient chain process for the destruction of $HO_2\cdot$ and would therefore result in no longer-lived $HO_2\cdot$, inconsistent with the data. However, it cannot be excluded that the reaction occurs with a rate constant of 5×10^7 M^{-1} s^{-1} or less.

To check the consequences of reaction 18 for the decay of Cl_2^-, the course of Cl_2^- decay was also predicted by using the complete

(8) Eigen, M.; Kustin, K. *J. Am. Chem. Soc.* **1961**, *84*, 1355.
(9) Bielski, B. H. J. *Photochem. Photobiol.* **1978**, *28*, 645.
(10) Gear, C. W. *Commun. ACM* **1971**, *14*, 185.
(11) Bjergbakke, E.; Sehested, K.; Lang Rasmussen, O. *Radiat. Res.* **1976**, *66*, 433.

Table I

reaction	rate constant[a]	ref
(1) $H\cdot + O_2 \rightarrow HO_2\cdot$	2×10^{10}	3
(2) $H\cdot + H\cdot \rightarrow H_2$	2.2×10^{10}	3
(3) $H\cdot + \cdot OH \rightarrow H_2O$	1.5×10^{10}	3
(4) $H\cdot + HO_2\cdot \rightarrow H_2O_2$	1.3×10^{10}	3
(5) $\cdot OH + HO_2\cdot \rightarrow H_2O + O_2$	1.18×10^{10}	3
(6) $\cdot OH + \cdot OH \rightarrow H_2O_2$	1.2×10^{10}	3
(7) $HO_2\cdot + HO_2\cdot \rightarrow H_2O_2 + O_2$	2.1×10^{6}	3
(8) $OH + Cl^- \rightarrow OH^- + Cl\cdot$	4.3×10^{9}	4
(9) $H\cdot + H_2O_2 \rightarrow H_2O + \cdot OH$	6×10^{7}	5
(10) $Cl\cdot + Cl^- \rightarrow Cl_2^{-}\cdot$	2.1×10^{10}	4
(11) $Cl_2^{-}\cdot \rightarrow Cl\cdot + Cl^-$	1.1×10^{5}	4
(12) $Cl_2^{-}\cdot + Cl_2^{-}\cdot \rightarrow Cl_3^- + Cl^-$	4.0×10^{9}	1
(13) $Cl_2^{-}\cdot + HO_2\cdot \rightarrow 2Cl^- + H^+ + O_2$	1.0×10^{9}	1
(14) $Cl_2^{-}\cdot + H\cdot \rightarrow 2Cl^- + H^+$	7×10^{9}	1
(15) $H_2O_2 + Cl_2^{-}\cdot \rightarrow HO_2\cdot + 2Cl^- + H^+$	1.4×10^{5}	6
(16) $Cl_2 + Cl^- \rightarrow Cl_3^-$	1.8×10^{5}	7
(17) $Cl_3^- \rightarrow Cl_2 + Cl^-$	1.0×10^{6}	7
(18) $Cl_2 + HO_2\cdot \rightarrow Cl_2^{-}\cdot + H^+ + O_2$	see text	
(19) $Cl_3^- + HO_2\cdot \rightarrow Cl_2^{-}\cdot + Cl^- + H^+ + O_2$	see text	

[a] Rate constants for reactions of the type $R\cdot + R\cdot \rightarrow$ products are those defined by $-d[R\cdot]/dt = k[R\cdot]^2$. The units are $M^{-1}\ s^{-1}$ except for reactions 11 and 17 where they are s^{-1}.

reaction scheme 1-19. The fit shown in Figure 2 is good. By comparison with previous work,[1] it is clear that reaction 18 makes little difference to the decay of $Cl_2^{-}\cdot$.

We conclude that $HO_2\cdot$ reduces Cl_2 with $k = 1.0 \times 10^9\ M^{-1}\ s^{-1}$, i.e., close to the diffusion-controlled limit. The reaction may take place in various circumstances and should, for example, be considered together with some of the other reactions in Table I when formulating free-radical mechanisms for the reaction between H_2O_2 and Cl_2.[12,13]

Acknowledgment. This work was partly supported by grants from the Cancer Research Campaign and the Medical Research Council.

(12) Davies, G.; Kustin, K. *Inorg. Chem.* **1973**, *12*, 961.
(13) Held, A. M.; Halko, D. J.; Hurst, J. K. *J. Am. Chem. Soc.* **1978**, *100*, 5732.

Resonance Raman Evidence of Iron Pentacoordination in High-Spin Ferric Cytochrome P-450. A Comparison with Model Compound Iron(III) Protoporphyrin IX Dimethyl Ester *p*-Nitrobenzenethiolate

Pavel Anzenbacher,* Zdeněk Šípal, and Bohuslav Strauch[†]

Department of Biochemistry, Charles University Albertov 2030, 128 40 Prague 2, Czechoslovakia

Jacek Twardowski and Leonard M. Proniewicz[‡]

Institute of Zoology, Jagellonian University Karasia 6, 30060 Cracow, Poland

Received March 4, 1981
Revised Manuscript Received July 6, 1981

The resonance Raman (RR)[1] spectra of biomolecules provide an unique in situ insight into the stereochemistry of these substances.[2-4] Recently, Spiro et al.[5] reported in this journal a well-documented analysis of RR spectra of various heme proteins and their model substances. These data demonstrate that from the positions of high-frequency RR bands information about heme coordination and porphyrin core expansion can be drawn. As has been shown by structural studies, the central iron atom in high-spin ferric porphyrin complexes may be either five- or six-coordinated.[6,7] Spiro et al.[5] have presented reasoning which allows one to check the probability of iron penta- or hexacoordination in this class of heme compounds. Similar conclusions were reached also by Sievers et al.[8] The data presented in ref 5 support previous suggestions that porphyrin core expansion is responsible for the decrease of RR band frequencies of heme compounds (Spaulding et al.[9], Huong and Pommier[10]). From the position of spin-sensitive RR bands (marked II, IV, and V[11]), a porphyrin center-to-pyrrole nitrogen distance (C_t-N) can be calculated from the equation[5,10] $\nu = KA - Kd$, where d is the C_t-N distance in Å, ν the Raman shift frequency in cm^{-1}, and the constants K (cm^{-1}/Å) and A (Å) are 375.5 and 6.01 for band II, 555.6 and 4.86 for band IV, and 423.7 and 5.87 for band V, respectively. These relations were used to probe heme expansion in various heme proteins and model complexes.[5,9,10,12] The correlation for band V has been found to be less satisfactory due to contributions from various porphyrin-ring-stretching vibrations.[12a]

This procedure can be applied to the interpretation of the RR pattern of cytochrome P-450, a heme protein acting as a terminal oxidase in monooxygenation of a variety of both foreign and endogeneous substrates.[13] For a better understanding of its mode of action, the question of axial ligands of heme iron atom is of paramount importance. There is a strong indirect evidence of

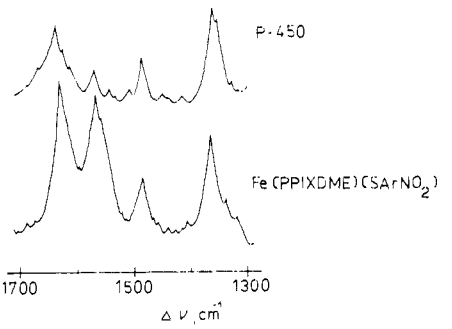

Figure 1. RR spectra of rat LM HS P-450 and model substance Fe(PPIXDME)($SArNO_2$). Model compound prepared according to ref 15. For preparation of P-450, see original work.[16c] Excitation wavelength, 488.0 nm; average incident power, 100 mW. Rat LM HS P-450: Jeol JRS S1 spectrometer, slit width 8.4 cm^{-1}, scan rate 60 cm^{-1}/min, sample in capillary (see ref 16c); Fe(PPIXDME)($SArNO_2$): Cary 82 spectrometer, slit width 7 cm^{-1}, scan rate 36 cm^{-1}/min, sample with KBr (1:1 w/w).

[†] Department of Inorganic Chemistry.
[‡] Central Laboratory for Physicochemical Analyses and Structural Research.

(1) Abbreviations used: RR, resonance Raman; P-450, Cytochrome P-450; HS, high spin; LS, low spin; Fe(PPIXDME)($SArNO_2$), iron(III) protoporphyrin IX dimethyl ester *p*-nitrobenzenethiolate; LM, liver microsomes; cam, P-450 from bacteria *Pseudomonas putida* grown on camphor; HRP, horseradish peroxidase; $(Me_2SO)_2$Fe(PPIX), bis(dimethyl sulfoxide) iron(III) protoporphyrin IX dimethyl ester; $(Me_2SO)_2$Fe(OEP), its octaethylporphyrin analogue; MetHb, methemoglobin; $(Im)_2$Fe(MP), bis(imidazole)iron(III) mesoporphyrin.

(2) Spiro, T. G. *Biochim. Biophys. Acta* **1975**, *416*, 169-189.
(3) Warshel, A. *Annu. Rev. Biophys. Bioeng.* **1977**, *6*, 273-300.
(4) Carey, P. R. *Q. Rev. Biophys.* **1978**, *11*, 309-370.
(5) Spiro, T. G.; Stong, J. D.; Stein, P. *J. Am. Chem. Soc.* **1979**, *101*, 2648-2655.
(6) Zobrist, M.; LaMar, G. N. *J. Am. Chem. Soc.* **1978**, *100*, 1944-1946.
(7) Mashiko, T.; Kastner, M. E.; Spartalian, K.; Scheidt, W. R.; Reed, C. A. *J. Am. Chem. Soc.* **1978**, *100*, 6354-6362.
(8) Sievers, G.; Österlund, K.; Ellfolk, N. *Biochim. Biophys. Acta* **1979**, 581, 1-14.
(9) Spaulding, I. D.; Chang, C. C.; Yu, N.-T.; Felton, R. H. *J. Am. Chem. Soc.* **1975**, *97*, 2517-2525.
(10) Huong, P. V.; Pommier, J. C. *C. R. Hebd. Seances Acad. Sci., Ser. C* **1977**, *285*, 519-522.
(11) Spiro, T. G.; Burke, J. M. *J. Am. Chem. Soc.* **1976**, *98*, 5482-5489.
(12) (a) Lanir, A.; Yu, N.-T.; Felton, R. H. *Biochemistry* **1979**, *18*, 1656-1660. (b) Asher, S. A.; Schuster, T. M. *Ibid.* **1979**, *18*, 5377-5387. (c) McCandlish, E.; Miksztal, A. R.; Nappa, M.; Sprenger, A. Q.; Valentine, J. S.; Strong, J. D.; Spiro, T. G. *J. Am. Chem. Soc.* **1980**, *102*, 4268-4271. (d) Campbell, J. R.; Clark, R. J. H.; Clore, G. M.; Lane, A. N. *Inorg. Chim. Acta* **1980**, *46*, 77-84. (e) Armstrong, R. S.; Irwin, M. J.; Wright, P. E. *Biochem. Biophys. Res. Commun.* **1980**, *95*, 682-689.
(13) (a) Estabrook, R. W. *Methods Enzymol.* **1978**, *52*, 43-47. (b) Gunsalus, I. C.; Sligar, S. G. *Adv. Enzymol.* **1978**, 47, 1-44. (c) White, R. E.; Coon, M. J. *Annu. Rev. Biochem.* **1980**, *49*, 315-356.

0002-7863/81/1503-5928$01.25/0